A STUDY OF DIVERGENCE IN GRADIENT FLOW

BY
HALTON HAGEN TAYLOR

THESIS
T22

Library
U. S. Naval Postgraduate School
Annapolis, Md.

DUDLEY KNOX LIBRARY
NAVAL POSTGRADUATE SCHOOL
MONTEREY, CALIFORNIA 93943-5002

A STUDY OF DIVERGENCE IN GRADIENT FLOW

by
H. H. Taylor

A STUDY OF DIVERGENCE IN GRADIENT FLOW

by
Halton Hagen Taylor
Lieutenant, United States Navy

Submitted in partial fulfillment
of the requirements
for the degree of
MASTER OF SCIENCE
IN AEROLOGY

United States Naval Postgraduate School
Monterey, California
1950

This work is accepted as fulfilling
the thesis requirements for the degree of

MASTER OF SCIENCE
IN AEROLOGY

from the
United States Naval Postgraduate School

PREFACE

The purpose of this research was to examine the instantaneous divergence of the gradient wind at individual points in circular and sinusoidal isobaric patterns.

This work was conducted at the U. S. Naval Postgraduate School, Monterey, California, during the period December 1949 to May 1950.

I wish to express my appreciation to Professor William D. Duthie and to Associate Professor A. B. Newboorn for their advice and guidance throughout.

TABLE OF CONTENTS

		Page
CERTIFICATE OF APPROVAL		i
PREFACE		ii
TABLE OF CONTENTS		iii
LIST OF ILLUSTRATIONS		iv
TABLE OF SYMBOLS AND ABBREVIATIONS		v
INTRODUCTION		1
CHAPTER		
I.	THE MASS DIVERGENCE EQUATION	5
	1. Theoretical Derivation	5
	2. Qualitative Interpretation	7
	3. A Numerical Example	8
II.	THE VELOCITY DIVERGENCE EQUATION	12
	1. Derivation of Formula	12
	2. Qualitative Interpretation	13
	3. A Numerical Example	14
	4. Conclusions from the Variable Pressure Gradient Case	15
III.	NUMERICAL INVESTIGATIONS	18
	1. Moving Systems	18
	2. Conclusions from Moving Systems	20
	3. Investigation of Sinusoidal Waves	23
	4. Comparison of the Terms $\underline{v} \cdot \nabla v$ and $v \nabla \cdot \underline{v}$	24
IV.	SYNOPTIC ASPECTS	26
	1. Application to the Tendency Equation	26
	2. Theoretical Investigation of a Surface Low with a Sinusoidal Pattern Above	27
	3. Computation of $\underline{v} \cdot \nabla v$ and $v \nabla \cdot \underline{v}$ from Actual Charts	28
	4. Synoptic Evidences of Convergence or Divergence	29
BIBLIOGRAPHY		30

LIST OF ILLUSTRATIONS

		Page
Figure 1.	Stationary Circular Low with Constant Pressure Gradient	10
Figure 2.	Stationary Circular Low with Pressure Gradient a Function of Radius of Curvature of Isobars	16
Figure 3.	Pressure Profile for the Variable Pressure Gradient Case	17
Figure 4.	Plotting Method for Moving Pressure Systems	18
Figure 5.	Circular Low, with Constant Pressure Gradient, moving eastward 10 knots	21
Figure 6.	Circular Low, with Constant Pressure Gradient, moving eastward 30 knots	22
Figure 7.	Sign of $\mathbf{t} \cdot \nabla V$ in Wedges and Troughs of Sinusoidal Isobars	24
Figure 8.	Sign of $V \nabla \cdot \mathbf{t}$ in Wedges and Troughs of Sinusoidal Isobars	24
Table 1.	Values of Divergence at Various Points on a Stationary Circular Low with Constant Pressure Gradient	9
Table 2.	Values of Divergence at Various Points on a Stationary Circular Low with Pressure Gradient a Function of Radius of Curvature of Isobars	15
Table 3.	Values of Divergence at Various Points on a Circular Low, with Constant Pressure Gradient, moving eastward 10 knots	20
Table 4.	Relative Values of $\mathbf{t} \cdot \nabla V$ and $V \nabla \cdot \mathbf{t}$ in Sinusoidal Isobars	25
Table 5.	Total Contributions of Frictional and Divergence Layers to the Surface Pressure Tendency for a Particular Low	27
Table 6.	Contribution of Divergence to Surface Pressure Tendency as Computed from Actual Charts	28

PLATE

(Inside back cover)

I. Isovel Pattern for Stationary Sinusoidal Isobars

TABLE OF SYMBOLS AND ABBREVIATIONS

X

Y

π

Standard mathematical definitions

unless otherwise noted

$\underline{i}$

$\underline{j}$

$\underline{k}$

$\nabla = \frac{\partial}{\partial x}\underline{i} + \frac{\partial}{\partial y}\underline{j}$

∇p

$|\nabla p|$

$\frac{dy}{dx}$

$\frac{d^2y}{dx^2}$

$\underline{V}$ - Gradient wind vector

$\underline{V}_{gs}$ - Geostrophic wind vector

v - Gradient wind speed

p_o - Atmospheric pressure at the surface of the earth

λ - Coriolis parameter

ρ - Density

g - Acceleration due to gravity

w - Vertical component of the wind

K - Curvature of trajectory of air particle

K_i - Curvature of isobar

C - Speed of pressure system

N - $(\lambda + \nu K)^{-1}$

$\underline{t}$ - Unit vector parallel to the wind

t - Time

ψ - Angle between direction of movement of pressure system and direction of isobar at a point

R_i - Radius of curvature of isobar

A_i - Amplitude of isobar

L_i - Wave length of isobar

B - $2\pi (L_i)^{-1}$

θ - Latitude

a - Radius of the earth

ω - Angular speed of the earth

$\frac{\partial p}{\partial R_i}$ - Local change of pressure with respect to radius of curvature of isobars

$\frac{\partial p_i}{\partial t}$ - Local rate of change of pressure at an arbitrary level

$\frac{\partial p_o}{\partial t}$ - Local rate of change of pressure at the surface of the earth

ΔY - Distance north or south of center of isobar

INTRODUCTION

The variation of pressure with time in any meteorological situation has long been recognized as one of the basic foundations upon which prognosis and forecast must rely. As a result, a considerable amount of meteorological literature has been devoted to the tendency equation in its various forms. Both the advection term and the divergence term have been extensively investigated from the theoretical standpoint. Petterssen [9] in a recent paper devised a simple method for quantitative evaluation of the advection term. As yet no such method has been devised for the divergence term. Bjerknes and Holmboe [4] considered mass divergence instead of investigating the two terms separately (as is done here). Their approach was dynamic in nature, being associated with the equations of motion and isobars or isohypses on upper-level maps.

Most investigations of this subject have considered the average distribution of divergence over an area. A study of the instantaneous velocity divergence in circular and sinusoidal patterns is considered here, and points as well as areas of convergence and divergence compared.

The first chapter deals with a derivation and a brief qualitative discussion of mass divergence. The numerical example, however, considers density a constant, thereby giving the product of density times the divergence of the gradient wind. Throughout the following, unless mass divergence is specifically specified, velocity divergence is intended. Likewise, only horizontal divergence is being considered in this study.

Horizontal divergence of any vector-field is a scalar function of position and time. At a fixed time therefore, horizontal divergence is a function of position alone. Thus, if the vector-field $\vec{V}$ is known at time (t), say at the time of the weather map, the divergence may be determined from the vector-field at that time. The horizontal divergence in this investigation is broken down into two parts: (1) the wind-speed times the divergence of the unit-vector tangent to the horizontal streamlines; and (2) the scalar product of the unit-tangent vector and the gradient of the horizontal wind-speed. Five different isobar patterns are investigated: (1) stationary circular low with constant pressure gradient; (2) circular low, with constant pressure gradient, moving eastward 10 knots; (3) circular low, with constant pressure gradient, moving eastward 30 knots; (4) stationary circular low with pressure gradient a function of radius of curvature of isobars; and (5) sinusoidal waves. Horizontal divergence is computed at various points in each of the patterns and the relative magnitudes noted. In all the circular cases investigated, there is convergence to the east of the meridian running through the center and divergence to the west. The areas of maximum convergence and divergence are on the innermost isobars along the latitude circles through the center. The areas of instantaneous convergence and divergence are qualitatively the same as the areas of average convergence and divergence as stated by Bjerknes and Holmboe [4]. The general areas of maximum and minimum convergence and divergence in circular lows are in qualitative agreement with the findings of Petterssen [8, pp. 236-237].

A theoretical example is computed using a circular low at the surface with various average sinusoidal waves aloft. The changes in the contributions to the surface pressure tendency with the different wave patterns aloft are recorded in Table 5.

An investigation of the circular systems in this study shows that the isovels bear a close relationship to the critical eccentricity stated by Bjerknes and Holmboe [4] for circular systems. This would be expected however, since the isovels are lines of constant $(\lambda + v\kappa)^{-1}$, which is proportional to the transport capacity of isobaric channels as stated by Bjerknes and Holmboe [4].

A computation from the 850, 700, 500 and 300 millibar charts of 1500Z, 19 October, 1949 is made and the resulting contributions to the surface pressure tendency are compared with the observed tendencies. The order of magnitude of the contribution of the divergence term from the layers investigated is in agreement with the results of Baum [2].

Gradient flow is assumed throughout. The wind of course is not always gradient in nature even in the free atmosphere, although the latest investigations have shown that the difference between the gradient wind and the observed winds is usually very small at about 1000 meters above the ground. When the pressure gradient is changing rapidly, however, the relationship between the observed wind and the pressure gradient is considerably modified. This is due to the fact that the motion is then not under balanced forces. Under these conditions there is a velocity component along the isallobaric gradient. A computation of divergence assuming gradient flow in this case would generally be in error.

The synoptic evidences of convergence and divergence are discussed. In general it can be assumed that widespread cloudiness implies widespread convergence and clear skies imply divergence over the area.

I. THE MASS DIVERGENCE EQUATION

1. Theoretical derivation.

Let the wind be expressed in vector notation as

$$\underline{V} = \underline{V}_{gs} - \left(\frac{\nu K}{\lambda}\right)\underline{V} \tag{1.1}$$

Multiplying equation (1.1) by $\rho\lambda$ and collecting terms gives

$$(\lambda + \nu K)\rho\underline{V} = \lambda\,\rho\underline{V}_{gs} = -\nabla P \times \underline{K} \tag{1.2}$$

Solving equation (1.2) for $\rho\underline{V}$ we get

$$\rho\underline{V} = -\nabla P \times \underline{K}\,(\lambda + \nu K)^{-1} \tag{1.3}$$

Taking the horizontal divergence of both sides gives

$$\nabla\cdot\rho\underline{V} = -\nabla P \times \underline{K}\cdot\nabla(\lambda + \nu K)^{-1} + (\lambda + \nu K)^{-1}\nabla\cdot\nabla P \times \underline{K}$$

which reduces to

$$\nabla\cdot\rho\underline{V} = -\nabla P \times \underline{K}\cdot\nabla(\lambda + \nu K)^{-1} \tag{1.4}$$

since $\nabla\cdot\nabla P \times \underline{K} = 0$.

Equation (1.4) therefore gives the mass divergence or divergence of specific momentum in gradient flow as the scalar product of a vector parallel to the isobars and the gradient of the quantity $(\lambda + \nu K)^{-1}$.

Expansion of the right hand side of equation (1.4) gives

$$\nabla \cdot \rho \underline{V} = (\lambda + vK)^{-2} \nabla P \times \underline{K} \cdot \nabla (\lambda + vK) \qquad (1.5)$$

$$= (\lambda + vK)^{-2} \nabla P \times \underline{K} \cdot \nabla \lambda + (\lambda + vK)^{-2} \nabla P \times \underline{K} \cdot \nabla (vK) \qquad (1.6)$$

$$= \frac{\nabla P \times \underline{K} \cdot \nabla \lambda}{(\lambda + vK)^2} + \frac{\nabla P \times \underline{K} \cdot K \nabla v}{(\lambda + vK)^2} + \frac{\nabla P \times \underline{K} \cdot v \nabla K}{(\lambda + vK)^2} \qquad (1.7)$$

Since $\nabla \lambda$ is along a meridian, it may be written as $\nabla \lambda = \frac{\partial \lambda}{\partial y} \underline{i}$. Therefore, the first term on the right side of equation (1.7) can be further simplified. Making use of the fact that $y = a\theta$ and

$$\frac{\partial \lambda}{\partial y} \underline{i} = \frac{\partial}{\partial y} (2\omega \sin \theta)\, \underline{i}$$

$$= 2\omega \cos \theta \frac{\partial \theta}{\partial y} \underline{i}$$

$\nabla \lambda$ reduces to

$$\nabla \lambda = \frac{\lambda}{a} \cot \theta \underline{i} .$$

Equation (1.7) may therefore be written as

$$\nabla \cdot \rho \underline{V} = (a \tan \theta)^{-1} (\lambda + vK)^{-2} \lambda \nabla P \times \underline{K} \cdot \underline{i} + (\lambda + vK)^{-2} \nabla P \times \underline{K} \cdot K \nabla v$$

$$+ (\lambda + vK)^{-2} \nabla P \times \underline{K} \cdot v \nabla K . \qquad (1.8)$$

2. Qualitative Interpretation.

A qualitative examination of equation (1.6) shows that for straight parallel isobars running east west, the total mass divergence is exactly zero. The first term on the right hand side is zero because the two vectors are perpendicular; the second, because K is zero for straight isobars. If the isobars have any northward component, there is convergence, and any southward component, there is divergence. This convergence or divergence reaches a maximum when the isobars run due north or south, other things being equal.

Consider next the "Cartwheel", with ∇K equal to a constant. From equation (1.6), it can be seen that the complete divergence is given by the term $(\lambda+\nabla K)^{-2} \nabla P \lambda K \cdot \nabla \lambda$. Since $\nabla \lambda = \lambda (a)^{-1} \cot \theta$, the variation in divergence in middle latitudes for this case is largely determined by the direction and magnitude of the vector $\nabla P \lambda K$, for the variations in λ, a and $\cot \theta$ are very small. The area of convergence is to the east of the meridian through the center, and the area of divergence to the west. The magnitudes at points equatorward of the center are slightly larger than the values for corresponding points on the poleward side of the latitude circle through the center.

For a stationary circular low with constant pressure gradient, the numerator of the first term on the right side of equation (1.7) is zero on the meridian running through the center of the low, and reaches a maximum along the latitude circle through the center of the low if we neglect the very small variation of $\nabla \lambda$ in middle latitudes. It is negative to the eastward of the meridian through the center and positive to the westward

of the meridian. With density also a constant, the second term of (1.7), as will be seen from equation (1.10), is zero on the meridian through the center, reaches a maximum on the innermost isobar close to the latitude circle through the center, is negative to the eastward of the meridian through the center and positive to the westward of the meridian.

3. A Numerical Example.

For a numerical investigation of the stationary circular low with constant pressure gradient, isolines of the quantity $(\lambda + VK)^{-1}$ must be drawn. This is done in the following manner. Set

$$(\lambda+VK)^{-1} = \text{CONSTANT} = N$$
$$VK = \frac{1}{N} - \lambda \quad . \tag{1.9}$$

Substituting this value of VK in the gradient wind equation gives

$$\lambda V + V\left(\frac{1}{N} - \lambda\right) = \frac{1}{\rho}\frac{\partial P}{\partial N}$$
$$V = N\left(\frac{1}{\rho}\frac{\partial P}{\partial N}\right) \quad . \tag{1.10}$$

With constant pressure gradient and the variation of density in the horizontal neglected, the isolines of $(\lambda + VK)^{-1}$ are isovels, and are labeled with the appropriate value of the wind speed in Figure 1. Choosing an isovel to be plotted (10 meters per second for example), the corresponding value of N can be computed from equation (1.10). With V and N known, assigning the values of λ that occur in the low will determine the correct values of K: . These λ and K: values can then be plotted on the system using latitude circles and radii of curvature of isobars as coordinates. Connecting this series of points will give the isovel desired. The isovels

constructed for the stationary circular case are shown in Figure 1. From Figure 1 it is seen that there is convergence to the eastward and divergence to the westward of the meridian through the center, and the maximum areas of convergence and divergence are on the innermost isobars along the latitude circles through the center. Table 1 gives the relative values of divergence computed at the positions indicated in Figure 1.

Position	Value of Divergence x 10^5
A	-.31
B	-.22
C	-.52
D	-.13
E	.15
F	.22
G	.35
H	.08

TABLE 1.

Since density is considered constant in this computation, equation (1.4) no longer gives mass divergence but the product of density times the divergence of the gradient wind.

Figure 1 shows an interesting comparison with the theory of Bjerknes and Holmboe [4] on the critical eccentricity necessary for a stationary low. Their results showed that a stationary low with exactly the critical eccentricity for all isobaric channels would have almost concentric isobars near the center and increasingly eccentric isobars toward the periphery. A glance at Figure 1 shows that the isovels have almost exactly this distribution. We would expect them to have this distribution, however, since the

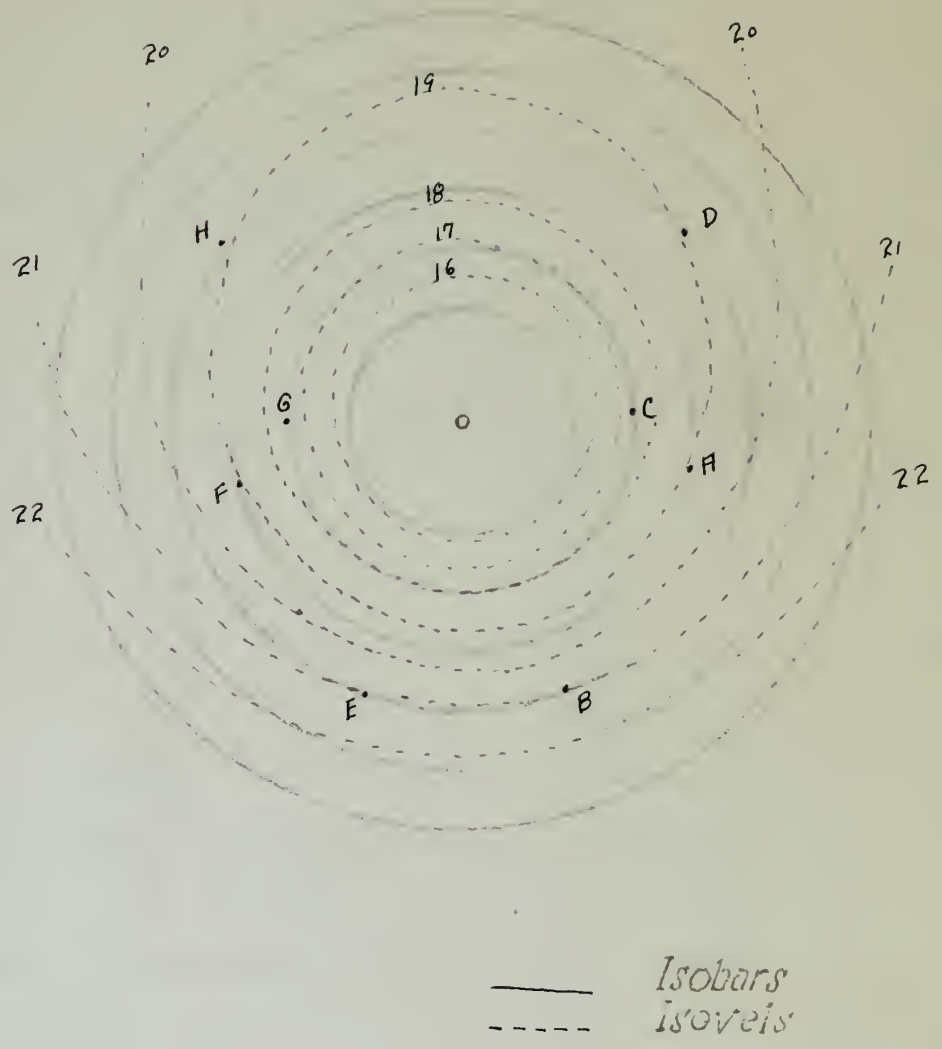

Figure 1.

isovels are lines of constant $(\lambda + VK)$, which, according to Bjerknes and Holmboe [4], are proportional to the transport capacity in gradient flow. Consequently, the isovels in Figures 1, 5 and 6 give the eccentricity of the isolines of equal transport capacity.

II. THE VELOCITY DIVERGENCE EQUATION

1. Derivation of Formula.

A glance at equation (1.10) shows that unless the pressure gradient is constant, isolines of the quantity $(\lambda + vK)^{-1}$ are not isovels. In order to determine the divergence from the isovels, the following notations were adopted. Set the wind equal to scalar v times vector $\underline{t}$ where $\underline{t}$ is defined as a unit vector parallel to the wind.

$$\underline{V} = v\,\underline{t} \tag{2.1}$$

$$\underline{t} = -\frac{\nabla P}{|\nabla P|} \times \underline{K} \tag{2.2}$$

The horizontal divergence of the wind may be written, by a simple vector-identity, as

$$\nabla \cdot \underline{V} = v \nabla \cdot \underline{t} + \underline{t} \cdot \nabla v \tag{2.3}$$

Equation (2.3) breaks the horizontal divergence down into two parts: (1) the wind speed times the divergence of the unit-vector tangent to the streamlines; and (2) the scalar product of the unit-vector tangent to the streamlines and the gradient of the horizontal wind speed.

Investigating the first term on the right side of equation (2.3), we find by substituting the value of $\underline{t}$ given in equation (2.2)

$$\begin{aligned} v\,\nabla \cdot \underline{t} &= -v \nabla \cdot \frac{\nabla P}{|\nabla P|} \times \underline{K} \\ &= -\frac{v}{|\nabla P|} \nabla \cdot \nabla P \times \underline{K} + \left(-v \nabla P \times \underline{K} \cdot \nabla \frac{1}{|\nabla P|}\right) \\ &= -v \nabla P \times \underline{K} \cdot \nabla \frac{1}{|\nabla P|} \end{aligned} \tag{2.4}$$

since $\nabla \cdot \nabla P \times \underline{K} = 0$.

Equation (2.4) may be further simplified by expanding the right hand term.

$$V\nabla\cdot\underline{t} = -V\nabla P\times\underline{K}\cdot\nabla\frac{1}{|\nabla P|} = V\nabla P\times\underline{K}\cdot\frac{\nabla|\nabla P|}{(|\nabla P|)^2}$$

$$= \frac{V\nabla P\times\underline{K}}{|\nabla P|}\cdot\frac{\nabla|\nabla P|}{|\nabla P|}$$

$$= -\underline{V}\cdot\frac{\nabla|\nabla P|}{|\nabla P|} \qquad (2.5)$$

2. Qualitative Interpretation.

Equation (2.5) shows that with a constant pressure gradient, the term $V\nabla\cdot\underline{t}=0$. A closer examination shows that for parallel isobars or for concentric circular isobars (not necessarily equally spaced) the term $V\nabla\cdot\underline{t}$ is still zero, since the gradient of $|\nabla P|$ is normal to the wind vector. For these three interesting cases then, the complete divergence of the wind is given by the term $\underline{t}\cdot\nabla V$.

$V\nabla\cdot\underline{t}$ essentially measures the spreading or closing of the isobars as can be seen from equation (2.5). With isobars spreading downwind, the term $V\nabla\cdot\underline{t}$ is positive, giving a negative contribution to the pressure tendency. This is in agreement with Scherhag's divergence theorem as stated by Baum [2] , that a horizontal flow divergence aloft is more frequently associated with pressure falls than with pressure rises below.

Examination of the second term of equation (2.3) shows that it is also related to the spreading or closing of the isobars. In general it is of opposite sign from the term $V\nabla\cdot\underline{t}$. Therefore, the two terms tend to cancel each other, and the total contribution to the pressure tendency is the residue.

Neither term by itself then gives a complete picture of the divergence unless the other term is zero. $V\nabla\cdot\underline{t}$ is zero for ∇p constant, parallel isobars or concentric circular isobars. $\underline{t}\cdot\nabla V$ is zero when the gradient of wind speed is normal to the wind direction. In these restricted cases, the complete divergence is given by the appropriate term in equation (2.3).

3. A Numerical Example.

A stationary circular low with the pressure gradient a function of radius of curvature of the isobars is constructed.

The gradient wind is a function of four variables: λ, ρ, R_i, and ∇p. Density has been considered constant in the horizontal throughout this investigation. Therefore, the wind can be written as

$$V = f\left(\lambda, R_i, \frac{\partial p}{\partial R_i}\right) \tag{2.6}$$

Since the low under consideration here is constructed with the pressure gradient a function of radius of curvature of the isobars, equation (2.6) reduces to

$$V = F(\lambda, R_i) \tag{2.7}$$

For plotting isovels therefore, choosing the value of V for the desired isoline and assigning values to R_i, determines the corresponding values for λ. With values of λ and R_i determined, the isovel is drawn by connecting the points by a smooth curve. Figure 2 shows the results of the computations. Figure 3 is the pressure profile of the low under consideration.

4. Conclusions from the Variable Pressure Gradient Case.

Figure 2 shows that the areas of convergence and divergence are the same as in the previous case, with convergence to the east and divergence to the west. The relative magnitudes changed, however. The computed values of the convergence to the east of the system were larger than those computed in the previous case. Table 2 gives the relative values of divergence computed at the positions indicated in Figure 2.

Position	Value of Divergence x 10^5
A	-.08
B	-1.5
C	-.15
D	.11
E	.52

TABLE 2.

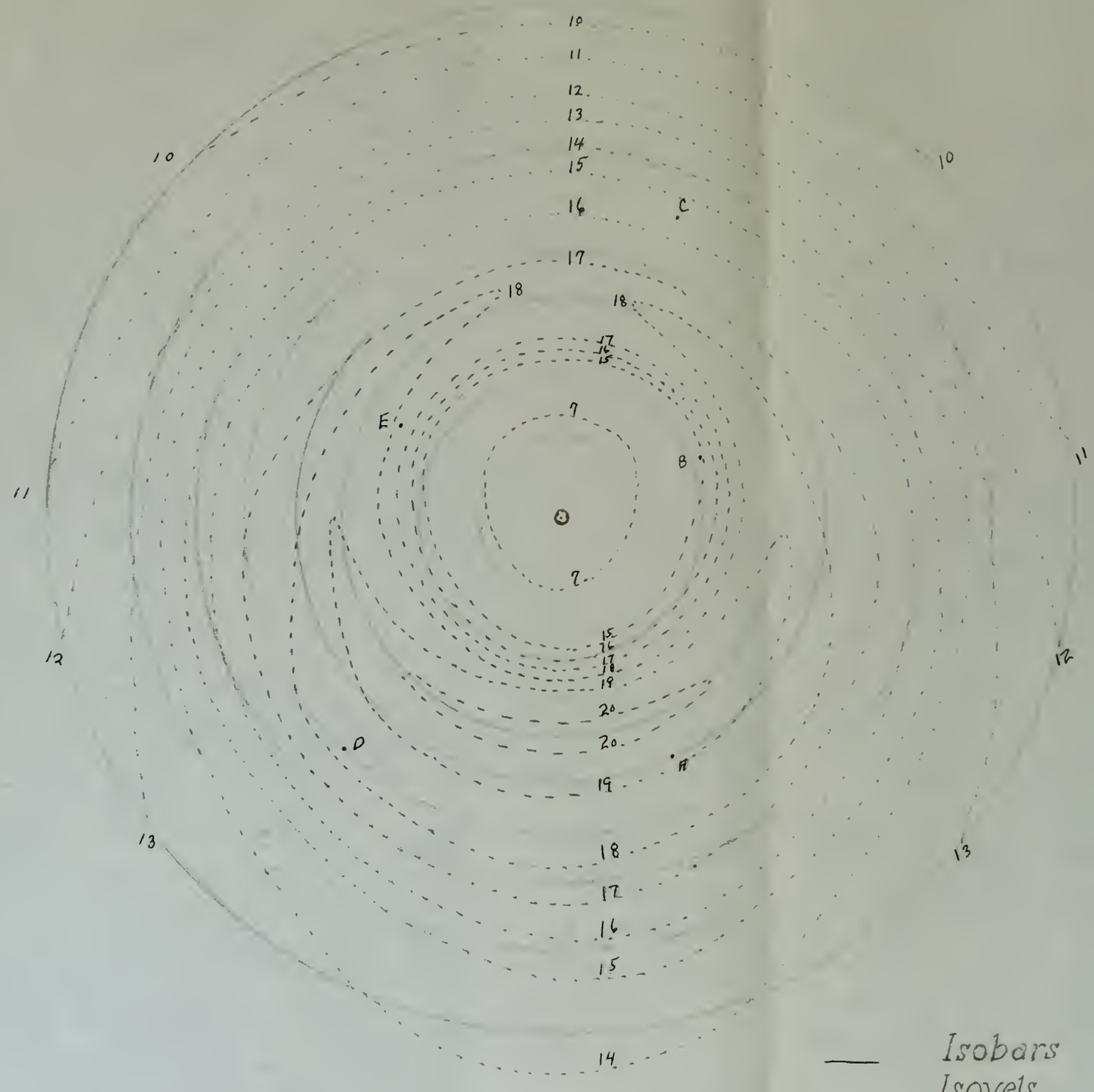
10
11
12
13
14
15
16
17
18
18
17
16
15
7
7
15
16
17
18
19
20
20
19
18
17
16
15
14
10
10
11
11
12
12
13
13
A
B
C
D
E
Isobars
Isovels

Figure 2.

——— *Isobars*

----- *Isovels*

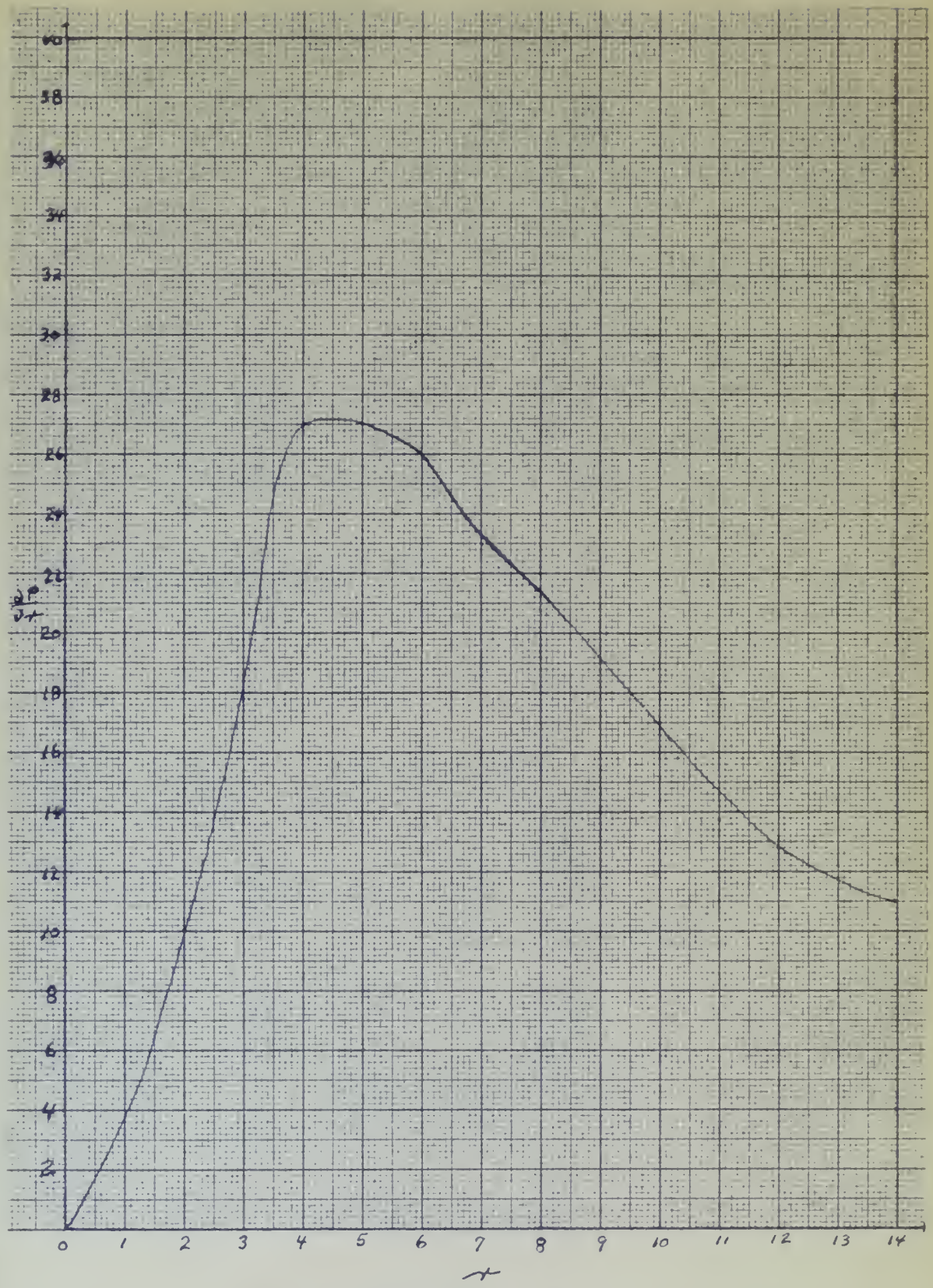

Figure 3.

III. NUMERICAL INVESTIGATIONS

1. Moving Systems.

Isovels are again plotted to determine quantitative values of divergence in a low. A circular low with constant pressure gradient is constructed. Eastward movements of 10 and 30 knots are considered.

Since the K appearing in equation (1.4) is the curvature of the trajectory of the air particle, it is necessary to relate it to the curvature of the isobars for plotting purposes. If the x-axis is chosen along the path of the center, and angle ψ is the angle between the x-axis and the wind direction, then from Petterssen [8] the desired relationship is

$$K = K_i \left(1 - \frac{c}{v} \cos\psi\right) \qquad (3.1)$$

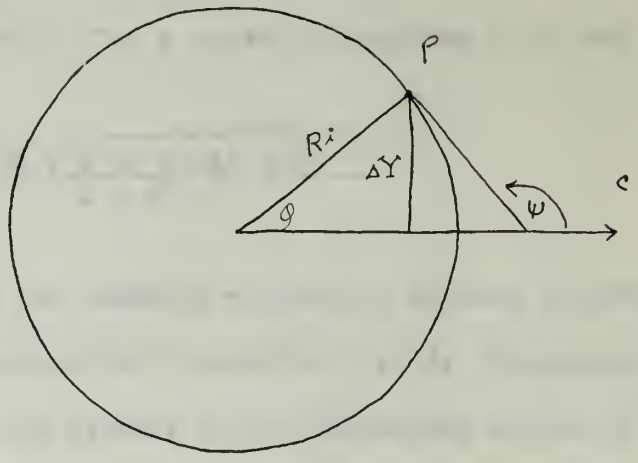

Figure 4.

To simplify plotting, the following method was derived. Take an arbitrary point P on an arbitrary isobar (Figure 4.). The line connecting P and the center of the isobar is R_i. Draw a line from the center of the isobar in the direction of movement of the system. Construct a tangent to the isobar at point P and extend the tangent line until it intersects the line in the direction of movement of the system. The angle between these two lines is then, by definition, angle Ψ. Let ΔY, measured in meters, represent the distance that point P is north or south of the center of the isobars. Then, by trigonometry,

$$\Delta Y = R_i \sin \varphi = R_i \sin (\psi - 90)$$

$$= \frac{1}{K_i} \sin (\psi - 90)$$

$$= -\frac{1}{K_i} \cos \psi$$

$$\cos \psi = -K_i \Delta Y \qquad (3.2)$$

Substituting the value of $\cos \psi$ above in equation (3.1) and solving gives

$$R_i = \frac{V \pm \sqrt{V^2 + 4VKC\Delta Y}}{2VK} \qquad (3.3)$$

In order to plot the isovels, a value is assumed (10 MPS for example) which determines a value of N in equation (1.10). Then choosing the values of λ that appear in the system, the corresponding values of K could be determined. The correct values of λ and R_i could then be computed from equation (3.3).

2. Conclusions from Moving Systems.

Figures 5 and 6 represent eastward moving systems with speeds of 10 and 30 knots respectively. Increasing the eastward movement of the system increases the gradient of v in the southern portion of the system and decreases the gradient of v in the northern portion. Considering the changes of the vector field $\vec{V}$, this is what we would expect. Since the isobar patterns were identical, the directions in the vector field were not changed. The magnitudes, however, did undergo a change. In the southern portion of the system, the movement of the system added to the magnitude of the wind vector since it was in the same direction. In the northern portion, on the other hand, the movement of the system was opposite to the wind vector so deducted from it. The area of convergence is still to the east of the meridian through the center of the low and divergence to the west of the meridian.

The algebraic sign of equation (1.4) or (2.3) can be determined from a glance at Figures 1, 5 and 6. Where the isovels cross isobars toward higher pressure, there is convergence and where they go toward lower pressure, there is divergence. Table 3 gives the relative values of divergence computed at the positions indicated in Figure 5.

Position	Value of Divergence x 10^5
A	-.28
B	-.10
C	-.57
D	-.07
E	.21
F	.26
G	.29
H	.07

TABLE 3.

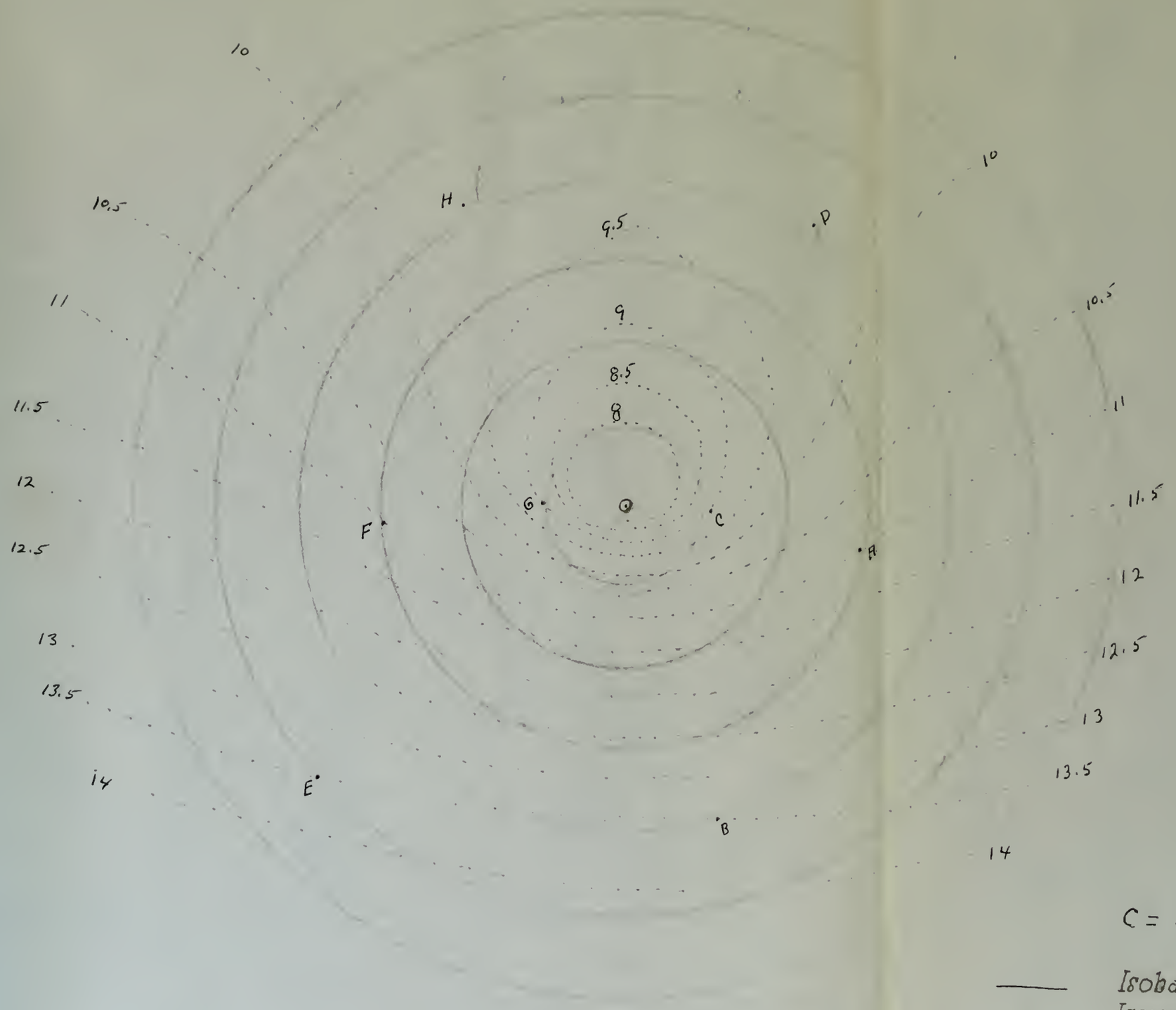
10
10.5
11
11.5
12
12.5
13
13.5
14
9.5
9
8.5
8
H
D
F
G
C
A
E
B
10
10.5
11
11.5
12
12.5
13
13.5
14
C = 10 KNOTS
Isobars
Isovels

Figure 5.

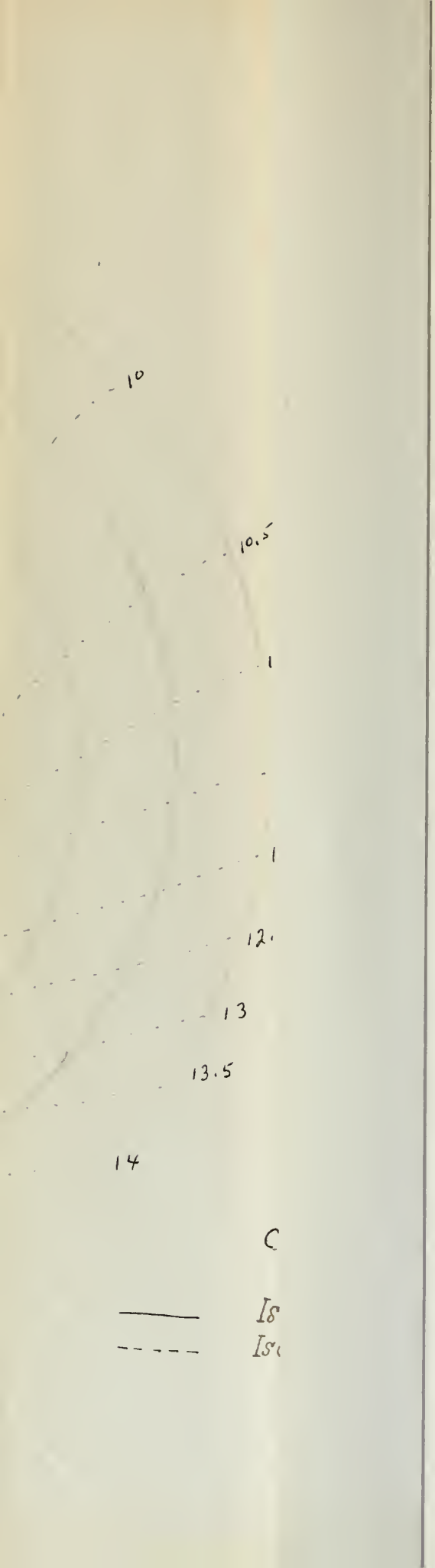
10
10.5
1
1
12
13
13.5
14
C
Is
Is

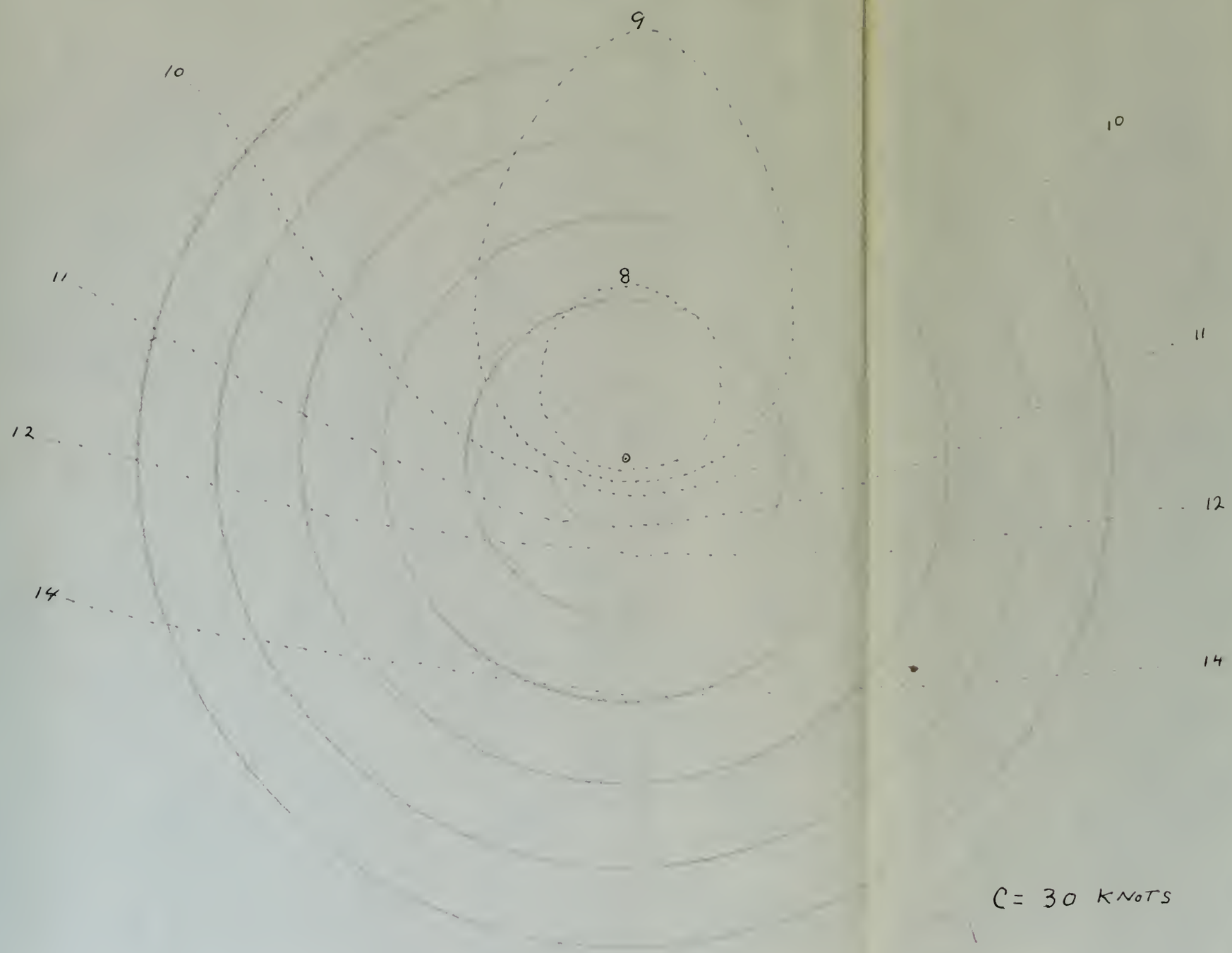

Figure 6.

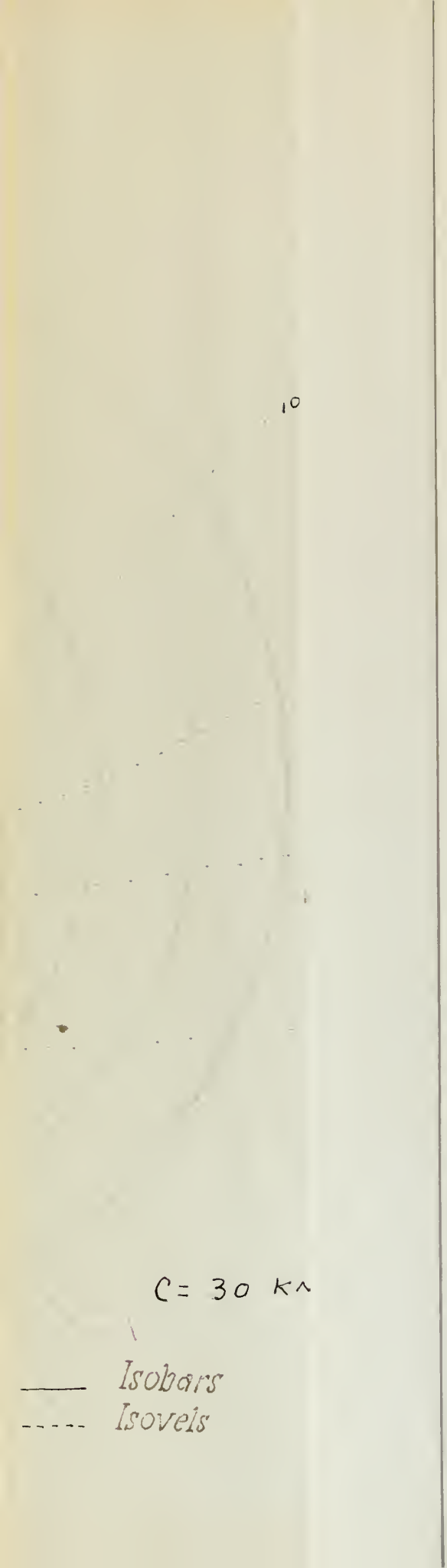
10
C = 30 K^
Isobars
Isovels

3. Investigation of Sinusoidal Waves.

Four sine waves are drawn displaced 180 nautical miles at the trough and wedge lines (Plate I.). Their wave length is 1800 nautical miles and their amplitude 660 nautical miles. Let the y-axis point northward and the x-axis point eastward. Then the equation of the sine wave may be given as

$$y = A_i \sin Bx \tag{3.5}$$

The curvature at any point on the sine wave is given by

$$K = \frac{\frac{d^2y}{dx^2}}{\left[1 + \left(\frac{dy}{dx}\right)^2\right]^{3/2}}$$

$$= -\frac{A_i B^2 \sin Bx}{\left[1 + (A_i^2 B^2 \cos^2 Bx)\right]^{3/2}} \tag{3.6}$$

The value of K is computed at 10° intervals along the east-west axis. Measuring the pressure gradient, and computing the value of λ at each of these points, the value of the gradient wind can be obtained from equation (3.7) for cyclonic curvature and equation (3.8) for anticyclonic curvature.

$$V = \tfrac{1}{2} \lambda R \left(\sqrt{1 + \frac{4 \frac{\partial p}{\partial N}}{\lambda^2 \rho R}} - 1 \right) \tag{3.7}$$

$$V = \tfrac{1}{2} \lambda R \left(1 - \sqrt{1 - \frac{4 \frac{\partial p}{\partial N}}{\lambda^2 \rho R}} \right) \tag{3.8}$$

Using the values of the wind computed at the various points, isovels are drawn as shown in Plate I.

4. Comparison of the Terms $\underline{v} \cdot \nabla v$ and $v \nabla \cdot \underline{v}$.

The algebraic sign of the term $\underline{v} \cdot \nabla v$ in wedges and troughs with sinusoidal isobars is given by Figure 7.

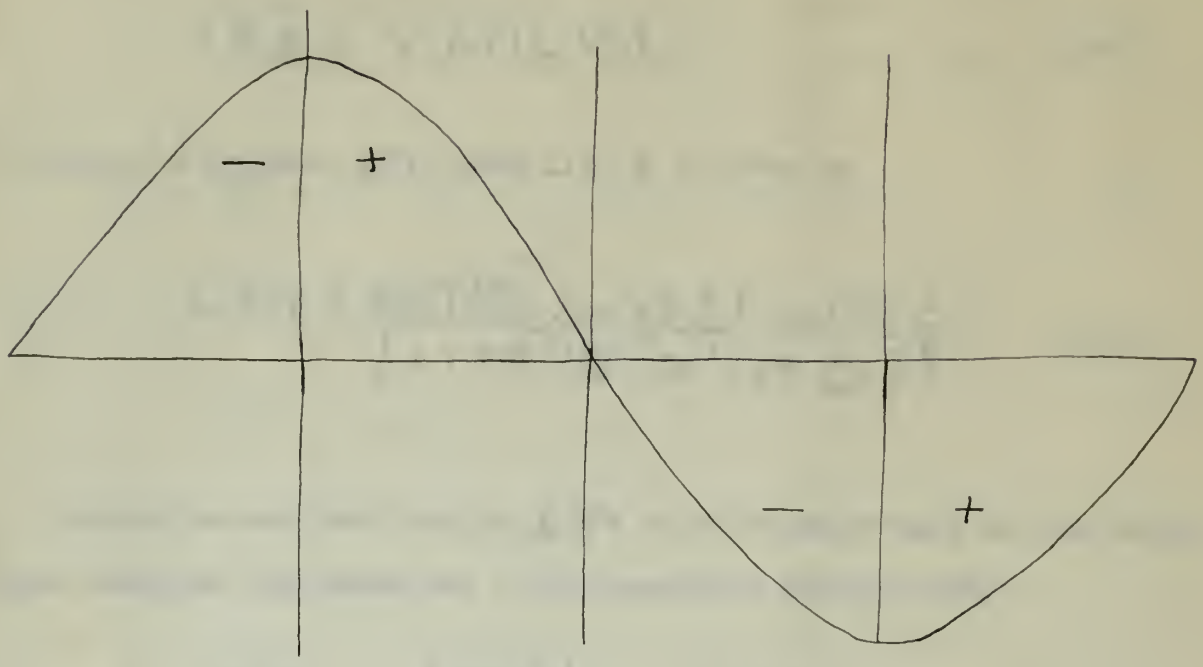

Figure 7.

Looking at the sign of $v \nabla \cdot \underline{v}$ in Figure 8, it is evident that the two terms tend to cancel each other since they are of opposite signs and are both related to the pressure gradient.

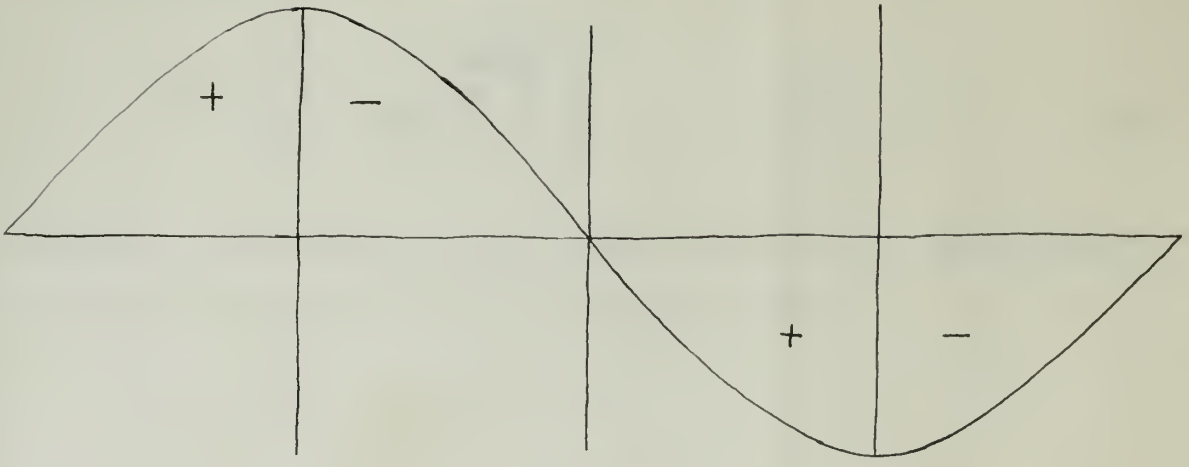

Figure 8.

The values of the two terms are computed at the points A, B, C, D and E on Plate I. $\nu\nabla\cdot\underline{t}$ is computed by the identity

$$\nu\nabla\cdot\underline{t} = \nu(L_i)^{-1}(L_i\nabla\cdot\underline{t}) \tag{3.9}$$

as suggested by Beers [3], where $L_i\nabla\cdot\underline{t}$ is given by

$$L_i\nabla\cdot\underline{t} = \frac{8\pi^3\left(\frac{L_i}{A_i}\right)^{-2} Sin\left(2\pi\frac{x}{L_i}\right) Cos\left(2\pi\frac{x}{L_i}\right)}{\left[1+4\pi^2\left(\frac{L_i}{A_i}\right)^{-2}Cos^2\left(2\pi\frac{x}{L_i}\right)\right]^{\frac{3}{2}}} \tag{3.10}$$

As can be seen from Table 4, $\underline{t}\cdot\nabla\nu$ is the dominant term in this particular case, but both terms are of the same order of magnitude.

Point	$\underline{t}\cdot\nabla\nu \times 10^5$	$\nu\nabla\cdot\underline{t} \times 10^5$
A	1.33	-1.07
B	.42	- .16
C	-1.26	.94
D	1.33	- .92
E	- .85	.61

TABLE 4.

IV. SYNOPTIC ASPECTS

1. Application to the Tendency Equation.

Petterssen [9, pp. 2-3], using the hydrostatic equation and the equation of continuity, derived the following for the tendency equation:

$$-\frac{\partial p}{\partial t} = \nabla p_1 \cdot \bar{V} + p \nabla \cdot \bar{V} - g \rho_1 w_1 \qquad (4.1)$$

which for sea level reduces to

$$-\frac{\partial p_0}{\partial t} = \nabla p_0 \cdot \bar{V} + p_0 \nabla \cdot \bar{V} . \qquad (4.2)$$

A quantitative evaluation of the first term on the right side of equation (4.1) was shown by Petterssen [9] to be fairly simple. Vector $\bar{V}$ is the isobaric-mean wind. It is obtained by observing the winds at equidistant pressure intervals (each isobaric layer containing the same amount of mass), summing, and dividing by the number of pressure intervals. The scalar product of this mean wind and the surface pressure gradient is then computed, giving the contribution of the transport term to the surface pressure tendency. The second, or divergence term, may be evaluated in a similar manner. Since

$$p_0 \nabla \cdot \bar{V} = p_0 \left[\bar{V}\, \overline{\nabla \cdot t} + \overline{t \cdot \nabla V} \right] \qquad (4.3)$$

evaluation of the right side of equation (4.3) gives the contribution of the divergence term to the surface pressure tendency.

2. Theoretical Investigation of a Surface Low with a Sinusoidal Pattern Above.

Consider a surface low, with an average cross-isobar flow of 15°, average wind speed (to the top of the friction-layer) of 30 knots, radius of curvature of isobar 180 nautical miles, and a friction-layer 100 mb thick. Then the contribution of the frictional inflow to the surface pressure tendency is approximately 12 millibars per 3 hours.

Next consider respectively the points A, B, C, D and E of Plate I as being the average divergence pattern for a thickness of 500 millibars above a point on the low being considered. Then Table 5 gives the total contribution of the two layers to the surface pressure tendency.

Millibars per 3 Hours

Point	Friction Layer	$\mathbf{k}\cdot\nabla V + V\nabla\cdot\mathbf{k}$	Total
A	12	-13.5	-1.5
B	12	-14.0	-2.0
C	12	17.2	29.2
D	12	-21.0	-9.0
E	12	13.0	25.0

TABLE 5.

3. Computation of $\underline{v} \cdot \nabla V$ and $V \nabla \cdot \underline{v}$ from Actual Charts.

The surface, 850, 700, 500 and 300 millibar charts of 1500Z, October 19, 1949 are used. Isovels are drawn on all the upper air charts as accurately as possible considering the scarcity of reports. The mean value of $\underline{v} \cdot \nabla V$ for the layers is then computed. Likewise, the mean value of $V \nabla \cdot \underline{v}$ is obtained. The contribution of the two terms to the surface pressure tendency is computed at six stations. Only stations with steady rising or falling tendencies are selected. The results are tabulated in Table 6.

mb per 3 Hours

Station	$\underline{v} \cdot \nabla V$	$V \nabla \cdot \underline{v}$	Total	Observed Surface Tendency
476	27	-45	-18	-1.9
469	47	-44	3	1.4
465	28	-23	5	2.5
413	-27	36	9	0.7
276	-19	7	-12	-0.8
666	-37	35	- 2	-0.5

TABLE 6.

The largest values of divergence in Table 6 are of the same order of magnitude as the findings of Baum [2] in his investigation of the relative sizes of the terms in the Baur and Phillip form of the tendency equation.

The quantitative investigation of the present series of maps shows that the upper air reports are neither numerous enough nor accurate enough for an

evaluation of the terms $\underline{v} \cdot \nabla V$ or $V \nabla \cdot \underline{v}$ on a quantitative basis. An error of only one meter per second in ∇V can give an error of approximately 10 millibars per 3 hours in the contribution of the term $\underline{v} \cdot \nabla V$.

4. Synoptic Evidences of Convergence or Divergence.

Generally, it may be said that divergence is associated with descending air and resultant clear skies, while convergence implies ascending air and condensation forms. Cyclonically curved and anticyclonically curved isobars aloft are frequently used to explain cloud forms and clear skies respectively. However, the mere fact of cyclonic or anticyclonic isobars does not imply either convergence or divergence above the friction layer, as can be seen by Figures 1, 2, 5 and 6. An absence of all cloud forms implies either very dry air or widespread divergence. Similarly, widespread cloudiness implies widespread convergence. The types that the cloud forms assume depend on the convective stability of the layers concerned in the lifting process. Thus stable air gives stratiform clouds while unstable air gives cumiliform clouds on being lifted. Many pilots, the author being one of them, have often wondered why the clouds are frequently spaced in the atmosphere in layers or sheets. When different levels of the atmosphere show different magnitudes of divergence or convergence, it follows that cloudiness will also exist in layers or sheets.

BIBLIOGRAPHY

1. Austin, J. M. Temperature Advection and Pressure Changes. Journal of Meteorology. 6: 358-360, October 1949.

2. Baun, W. A. Scherhag's Divergence Theorem. American Meteorological Society, Bulletin. 25: 319-326, October 1944.

3. Beers, N. R. Divergence of the Horizontal Wind. American Geophysical Union, Transactions. 26: 225-236, October 1945.

4. Bjerknes, J. and Holmboe, J. On the Theory of Cyclones. Journal of Meteorology. 1: 1-22, September 1944.

5. Granville, W. A., Smith, P. F., and Longley, W. R. Elements of the Differential and Integral Calculus. New York, Ginn and Co., 1941.

6. Haurwitz, B. Dynamic Meteorology. New York, McGraw-Hill, 1941.

7. Holmboe, J., Forsythe, G. E., and Gustin, W. Dynamic Meteorology. New York, John Wiley and Sons, 1945.

8. Pettersson, S. Weather Analysis and Forecasting. New York, McGraw-Hill, 1940.

9. Petterssen, S. Contribution to the Theory of Pressure Variations. Washington, Chief of Naval Operations, Aerology Section, May 1945.

10. Rossby, C - G. Kinematic and Hydrostatic Properties of Certain Long Waves in the Westerlies. Miscellaneous Reports Number 5. Chicago, University of Chicago, 1942.

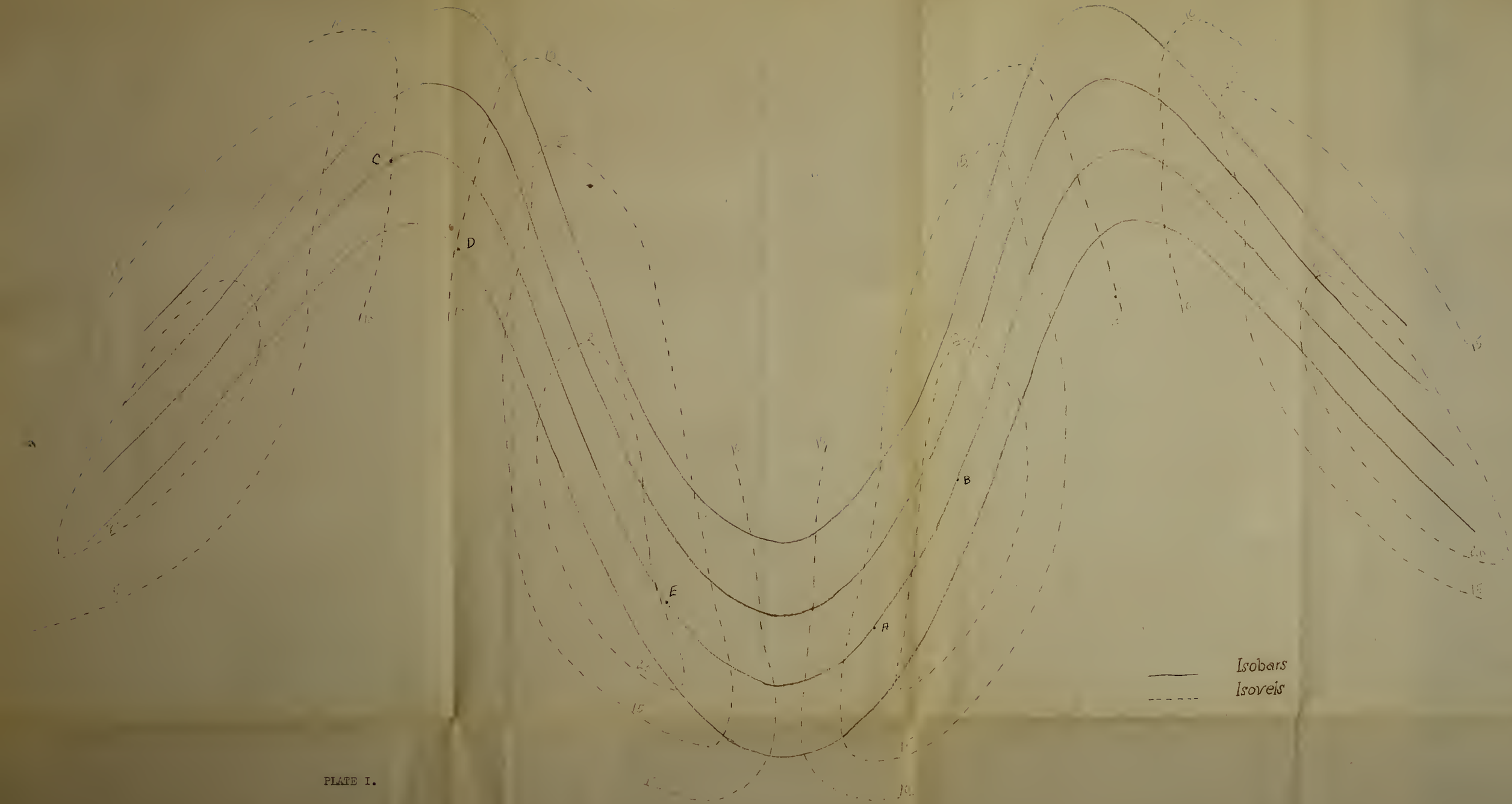

PLATE I.

APR 22 2nd T.L. (JBG) 7 6 5
3rd T.L.
JAN 16 4.T.L.
DEC 23
RENEWED
RENEWED

Thesis 13132
T22
Taylor, H. H.

AUTHOR

A study of divergence in gradi-

TITLE

ent flow.

DATE DUE	BORROWER'S NAME
JAN 30 '51	(illegible)

thesT22
A study of divergence in gradient flow.
3 2768 002 03396 1
DUDLEY KNOX LIBRARY